

True reentry of the glassy state in geometrically frustrated $\text{LiCr}_{1-x}\text{Mn}_x\text{O}_2$

S. Chattopadhyay, S. Giri, and S. Majumdar*

*Department of Solid State Physics, Indian Association for the Cultivation of Science,
2A & B Raja S. C. Mullick Road, Kolkata 700 032, INDIA*

D. Venkateshwarlu and V. Ganesan

UGC-DAE Consortium for Scientific Research, University Campus, Khandwa Road, Indore 452 017, INDIA

The development of spin glass like state in a geometrically frustrated (GF) magnet is a matter of great debate. We investigated the effect of magnetic (Mn) and nonmagnetic (Ga) doping at the Cr site of the layered GF antiferromagnetic compound LiCrO_2 . 10% Ga doping at the Cr site does not invoke any metastability typical of a glassy magnetic state. However, similar amount of Mn doping certainly drives the system to a spin glass state which is particularly evident from the relaxation, magnetic memory and heat capacity studies. The onset of glassy state in 10% Mn doped sample is of reentrant type developing out of higher temperature antiferromagnetic state. The spin glass state in the Mn-doped sample shows a true reentry with the complete disappearance of the antiferromagnetic phase below the spin glass transition. Mn doping at the Cr site can invoke random ferromagnetic Cr-Mn bonds in the otherwise 120° antiferromagnetic triangular lattice leading to the non-ergodic spin frozen state. The lack of spin glass state on Ga doping indicates the importance of random ferromagnetic/antiferromagnetic bonds for the glassy ground state in LiCrO_2 . Spin glass state in GF system has been earlier observed even for small non-magnetic disorder, and our result indicates that the issue is quite nontrivial and depends strongly on the material system concerned.

PACS numbers: 75.47.Lx, 75.50.Lk, 75.10.Jm, 75.40.Cx

I. INTRODUCTION

The term ‘Geometrical Frustration’ denotes a novel class of real systems where the arrangements of magnetic ions in the crystal lattice are such that the spins get frustrated in presence of conflicting exchange interactions resulting a complex magnetic state¹⁻³. On the other hand, ‘spin glass’ (SG) denotes a group of materials having metastable magnetic ground state associated with cooperative spin freezing in random fashion below a characteristic temperature T_f . SG is essentially a manifestation of chemical disorder along with frustration due to random as well as competing magnetic interactions⁴. Due to such proximity between SG and geometrically frustrated (GF) systems, sincere effort has been made in recent years to address an important issue, *i.e.* whether an SG like ground state can be realized in GF systems in presence of quenched disorder. As a result of rigorous investigations, spin freezing has been revealed in quite a few GF systems, such as $\text{SrCr}_8\text{Ga}_4\text{O}_{19}$, $\text{Gd}_3\text{Ga}_5\text{O}_{12}$, $\text{Y}_2\text{Mo}_2\text{O}_7$, $\text{Zn}_{1-x}\text{Cd}_x\text{Cr}_2\text{O}_4$, $\text{ZnCr}_{2-x}\text{Ga}_x\text{O}_4$ and so on⁵⁻⁹. Notably, some of these compositions show SG freezing even in their stoichiometric form where the amount of quenched disorder is supposed to be negligibly small. Thus, the origin of SG state in a GF material is widely debated, and different models have been proposed to account for that¹⁰. Apart from the origin, often the nature of the SG state in a GF material is found to be unusual. For example, the non linear susceptibility analysis on $\text{Tb}_2\text{Mo}_2\text{O}_7$ shows unconventional SG state in this chemically ordered GF compound¹¹. In case of doped GF sample such as $\text{SrCr}_{8.28}\text{Ga}_{3.72}\text{O}_{19}$, where sufficient chemical disorder is present, neutron scattering studies indicate that the

ground state magnetic excitation deviates significantly from that expected for a conventional SG¹². It is therefore appears that the SG state in a GF magnet is quite intriguing and there remains several open questions to be addressed.

Chemical substitution in a otherwise stoichiometric GF compound can create random exchange interaction through the breakage or alternation of magnetic bonds. It can also affect the magnetic interaction through the generation of random strains on substitution of atoms of different ionic radii¹⁰. The situation can be more complicated if the substituting atoms are magnetic in nature, as they can introduce additional magnetic interaction in the system. In this work we have investigated the role of chemical substitution (both magnetic and non-magnetic) on the magnetic ground state of LiCrO_2 .

LiCrO_2 is a well known GF magnet having layered hexagonal stacking along the c axis¹³⁻¹⁶. It is a quasi two dimensional magnetic oxide with extremely weak inter-layer interaction. Recently our group has reported the development of large electric polarization on Cu substitution at the Li site¹⁷ which is associated with enormous magneto-structural transition. The Cr^{3+} ions in LiCrO_2 remain within edge-sharing distorted CrO_6 octahedra and it results a layered arrangements of Cr ions separated by Li^+ and O^{2-} . The magnetic frustration in this compound arises due to triangular arrangements of Cr^{3+} ($S = 3/2$) ions in the basal plane coupled with each other through AFM type interaction. The compound shows a complex double-Q 120° AFM ordering below $T_N = 62$ K¹⁸, although the Curie-Weiss temperature is substantially high ($\theta_{CW} = -700$ K)¹⁶ resulting a large frustration factor $F = |\theta_{CW}|/T_N = 11.3$. The 2D

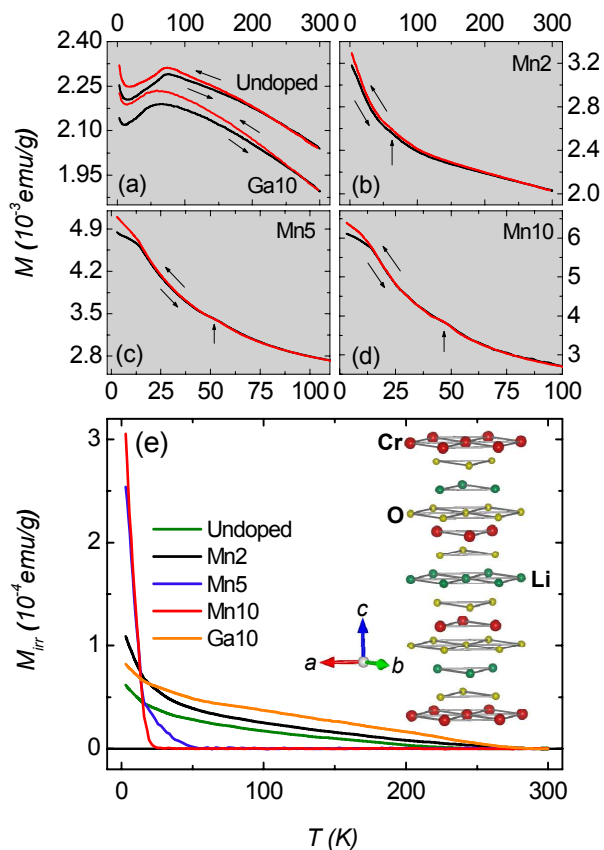


FIG. 1. Temperature (T) variation of magnetization (M) measured in zero field cooled (ZFC) and field cooled (FC) protocols with an applied field (H) of 100 Oe for (a) undoped and Ga10, (b) Mn2, (c) Mn5, and (d) Mn10 compositions. (e) shows the difference between FC and ZFC magnetization ($M_{irr} = M_{FC} - M_{ZFC}$) as a function of T for all of the compositions. Inset represents a perspective view of the crystal structure of LiCrO_2 .

triangular network in LiCrO_2 provides us a good opportunity to study the effect of chemical substitution on the magnetic ground state.

II. EXPERIMENTAL DETAILS

Polycrystalline samples of $\text{LiCr}_{1-x}\text{Mn}_x\text{O}_2$ ($x = 0.0, 0.02, 0.05, \text{ and } 0.1$, hereafter denoted by undoped, Mn2, Mn5, and Mn10 respectively) and $\text{LiCr}_{1-x}\text{Ga}_x\text{O}_2$ ($x = 0.1$, hereafter denoted by Ga10) were prepared as described elsewhere¹⁵. Powder x-ray diffraction (Cu K_α) was carried out on all the samples which are found to be single phase in nature having rhombohedral crystal structure (space group: $R\bar{3}m$). The estimated lattice parameters of the undoped sample are $a = 2.92 \text{ \AA}$ and $c = 14.43 \text{ \AA}$, which are very close to the previously reported values. DC magnetization (M) measurements were performed between 2 and 300 K using a Quantum Design SQUID magnetometer and a cryogen free high magnetic

TABLE I. Variation of the AFM onset temperature (T_p), ZFC-FC bifurcation temperature (T_{irr}), coercive field (H_C^{3K}) at 3 K, and difference between FC and ZFC magnetization (M_{irr}^{3K}) at 3 K for $\text{LiCr}_{1-x}\text{A}_x\text{O}_2$ ($A = \text{Ga, Mn}$).

Compositions	T_p (K)	T_{irr} (K)	H_C^{3K} (Oe)	M_{irr}^{3K} (10^{-4} emu/g)
Undoped	75	~ 250	–	0.6
Ga10	65	~ 285	–	0.8
Mn2	~ 54	~ 280	–	1.1
Mn5	~ 51	~ 50	~ 90	2.5
Mn10	~ 45	~ 20	~ 200	3.1

field system from Cryogenic Ltd., U.K. The heat capacity was measured on Quantum Design Physical Properties Measurement System using relaxation technique. Element mapping was performed in a high resolution transmission electron microscope (TEM) from JEOL.

III. RESULTS AND DISCUSSIONS

The T variation of M for doped and undoped samples is depicted in fig. 1. Measurements were performed in zero-field-cooled (ZFC) and field-cooled (FC) conditions under an applied magnetic field of 100 Oe. Both ZFC and FC curves of LiCrO_2 increase gradually below 300 K and show a peak around $T_p = 75 \text{ K}$ which signifies the onset of AFM transition as reported earlier¹³. Below 15 K, M shows a sharp upturn with decreasing T . Such upturn in low dimensional magnetic systems is often attributed to paramagnetic impurities and/or broken chain effect^{19,20}. A bifurcation between ZFC and FC curves appears below $T_{irr} \sim 250 \text{ K}$ for the pure sample. In LiCrO_2 , such irreversibility was reported earlier and it was attributed to the formation of *frozen magnetic clusters* having short range magnetic correlations¹³. On Ga doping (see the M - T curve of Ga10), the overall behavior of the thermomagnetic curve remains almost unaltered. Although, the peak becomes broader with a lowering of T_p (65 K). The magnitude of M decreases slightly in case of Ga-doped sample.

In contrary, Mn doping at the Cr site causes considerable change in the magnetic properties of LiCrO_2 . Figs. 1(b)-1(d) show ZFC and FC $M(T)$ curves of Mn2, Mn5, and Mn10 samples respectively, between 2 K and 300 K. A relatively weak hump like feature in all the doped samples can be observed in the ZFC or FC curves signifying the onset of the AFM transition. The anomaly is found to be around $T_p \sim 54 \text{ K}$, 51 K and 45 K for Mn2, Mn5, and Mn10 samples respectively. In Mn5 and Mn10, the low- T Curie tail-like rise is completely absent as well. The bifurcation point between FC and ZFC data gradually shifts to lower T with increasing Mn concentration (see table I). We have plotted $M_{irr} = M_{FC} - M_{ZFC}$ in fig. 1(e) to have a quantitative idea of the irreversibility in

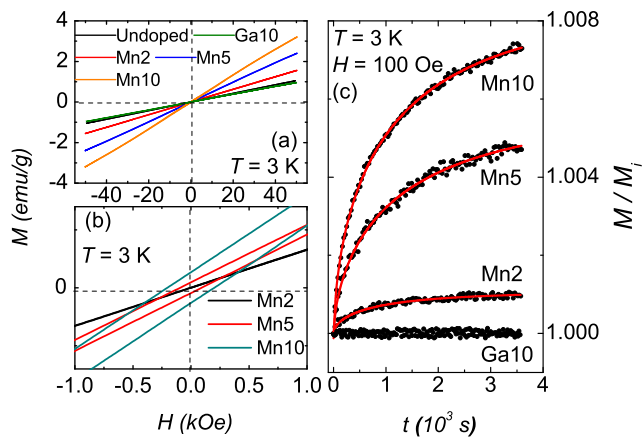


FIG. 2. (a) shows isothermal magnetization (M) as a function of applied magnetic field (H) for all the compositions at 3 K. (b) emphasizes the low field regime of M - H curves of Mn doped samples to depict the compositional variation of coercivity. (c) represents the time (t) variation of normalized M for Ga and Mn doped samples measured in zero field cooled condition at 3 K under an applied field of 100 Oe. Here, M_i denotes the initial magnetization in the beginning of measurement and solid lines are fit to the relaxation data with equation 1.

M . For undoped, Ga10 and Mn2 samples M_{irr} becomes non-zero below about 250 K, 285 K and 280 K respectively, whereas for Mn5 and Mn10 samples, it is negligibly small down to 50 K and 20 K respectively. However, below this temperatures M_{irr} rises sharply for Mn5 and Mn10 indicating large thermomagnetic irreversibility (see table I). Such low temperature rise in M_{irr} is absent in other samples and it signifies a different mechanism for the observed irreversibility in these two compositions.

Fig. 2(a) depicts isothermal field dependence of M at 3 K for all the samples. For the undoped and Ga10 samples, the M - H data is linear and does not show any hysteresis. This signifies strong AFM character. $M(H)$ of the Mn-doped samples show slight non-linearity especially at the high field region with curvature increasing with increasing Mn concentration. The magnitude of M is found to rise with Mn doping, while for 10% Ga doped sample it is almost same as of the undoped sample. Fig.2(b) emphasizes the low field region of $M(H)$ curves of the Mn doped samples. Interestingly, the presence of hysteresis can be observed in Mn5 and Mn10 compositions with a systematic enhancement of coercivity with Mn content (see table I).

An SG like state is generally characterized by a free energy landscape with innumerable numbers of nearly degenerate ground state configurations separated from each other by potential barriers of random height (landscape of random potential wells)²¹. A signature of such scenario is the presence of magnetic relaxation, which occurs due to the passage from one metastable state to another with time. Fig.2(c) depicts normalized M vs. time(t) data for the Mn and Ga doped samples at 3 K.

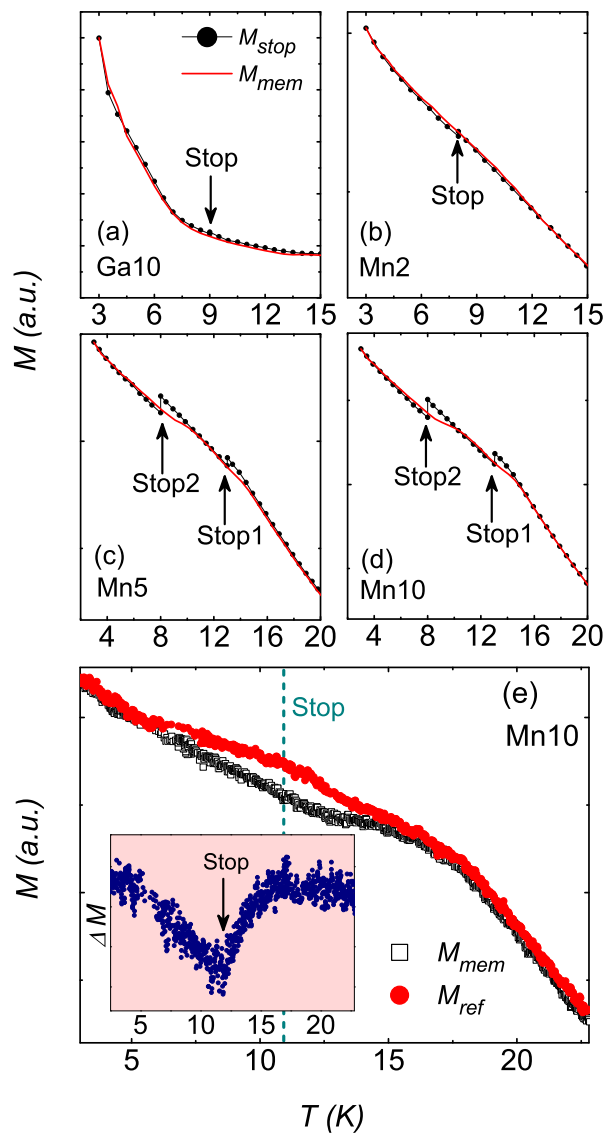


FIG. 3. (a)-(d) depict memory measurements following field stop field cooled protocol for Ga10, Mn2, Mn5, and Mn10 respectively with an applied field of 100 Oe. Here, M_{stop} denotes the cooling curve with stops of 3600 s each, and M_{mem} is the subsequent heating curve without any stop. (e) shows the ZFC memory measurement on Mn10. Where, M_{mem} represents the ZFC heating curve after the sample being cooled in zero field with an intermediate stop at 12 K for 18000 s. M_{ref} denotes the reference ZFC curve where the data was recorded during heating after the sample being cooled without any stop. Inset shows T dependence of the difference curve $\Delta M = M_{mem} - M_{ref}$ to illustrate the ZFC memory effect.

To record this data, samples were first zero field cooled from 300 K, and a field of 100 Oe was switched on. All the Mn-doped samples show the presence of finite relaxation with the magnitude getting higher with Mn concentration. However, we failed to observe any measurable relaxation in undoped and Ga10 sample. These relaxation

data in Mn-doped samples are found to be best described by a modified stretched exponential law²²⁻²⁵,

$$M(t) = M_i - M_r \exp[-(t/\tau)^\beta] \quad (1)$$

where, M_i is the initial magnetization, M_r is the amplitude of the metastable part, τ is the time constant and the parameter $0 \leq \beta \leq 1$ signifies the distribution of local energy minima. It approaches unity for a system with long range magnetic order. Fitting to the $M(t)$ data with this equation results $\beta = 0.64, 0.63, 0.60$ for Mn2, Mn5, and Mn10 respectively. The gradual decrease of the value of β signifies that the system passes through increased number of local minima in the energy landscape during relaxation. Systems having spin glass like ground states are found to show β ranging between $\sim 0.2-0.6$ ²⁶⁻²⁹. The estimated β values of the present compositions practically fall in this regime.

Evidently, the signature of metastability in Mn -doped samples are not visible in the undoped or Ga-doped samples. It thus seems that the magnetic ground state in nonmagnetic Ga-doped sample is different from that of magnetic Mn-doped counterparts. A possible way to distinguish a glassy metastable state from a long range ordered one is through magnetic memory measurements. We performed field stop field cool (FSFC) memory in $M(T)$ measurement on the Mn and Ga doped samples (see fig.3)^{30,31}. In this protocol, sample was first field cooled from 300 K down to 5 K with intermediate stops of 3600 s each with the magnetic field being reduced to zero during each stop (denoted as M_{stop}). After cooling, the samples were subsequently heated back to 300 K without any stop in presence of H (denoted as M_{mem}). A system with frozen/blocked spins (or spin clusters) is expected to show anomalies in the heating curve at the same temperatures where the sample was allowed to age during cooling. We do not observe any such anomalies in Ga10 and Mn2 samples (figs. 3 (a) and (b) respectively) at the stopping temperatures. On the other hand M_{mem} curves for Mn5 and Mn10 (figs. 3(c) and 3(d) respectively) show anomalies in M_{mem} with clear changes in slope at the stopping positions. The anomalies associated with the memory effect is found to be much stronger in Mn10 sample.

Although the existence of FSFC memory effect is a convincing signature of a frozen or blocked magnetic state, it cannot distinguish between a spin glass and superparamagnet. In order to resolve this issue, memory measurement in ZFC condition was performed on Mn10. Here the protocol remains almost the same as of FSSC barring the fact that the cooling was performed in zero field with a stop for 18000 s at 12 K. Fig. 3 (e) shows the subsequent heating curves (M_{mem}) along with the reference curves (M_{ref}), which is actually simple ZFC heating curve without any stop during cooling. The difference curve $\Delta M = M_{mem} - M_{ref}$ is plotted for Mn10 in the insets of fig. 3(e). Interestingly, M_{mem} and M_{ref} curves for Mn10 follows different path around the stopping temperature of

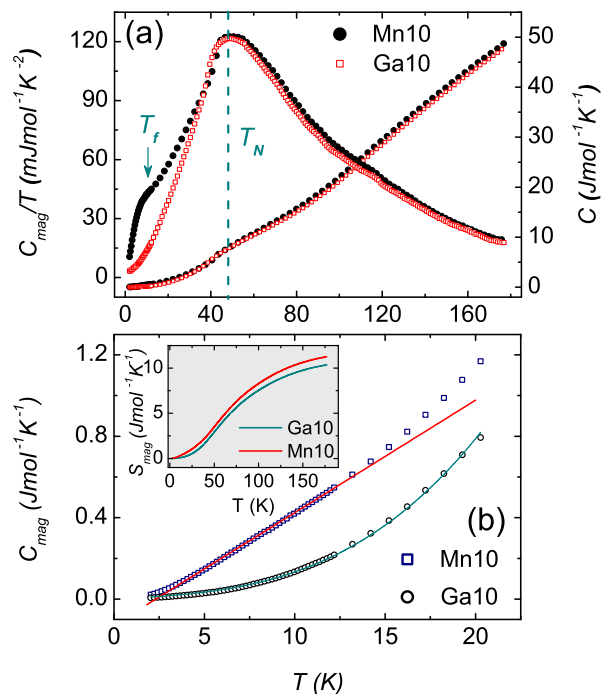


FIG. 4. (a) Right axis depicts temperature variation of the heat capacity (C) between 2 K and 180 K for Mn10 and Ga10 compositions. Whereas, the left axis represents variation of C_{mag}/T with temperature. Here, C_{mag} is the magnetic contribution of heat capacity. (b) shows the low- T side of C_{mag} for Mn10 and Ga10 as a function of T . Solid lines are the best fit to the data with appropriate algebraic expressions (see text for details). Inset shows T variation of magnetic entropy (S_{mag}) of both the samples.

12 K. This feature gets much more prominent in the difference curve as shown in the inset of fig. 3(e), where a dip can be seen with its minimum at $T_{stop} = 12$ K. The appearance of ZFC memory in Mn10 signifies that the substitution of Cr ions with Mn disrupts the AFM order and turns on a spin glass like magnetic ground state.

It is now pertinent to know the nature and origin of SG state in Mn10 sample, particularly to what extent it corresponds to a conventional SG state. We addressed this point through heat capacity (C) measurements on both Mn10 and Ga10 samples as depicted in fig. 4. In the C versus T data [see fig. 4(a)], a clear anomaly around 45 K is observed in both the samples which signifies the long range AFM transition. Apparently the C vs. T data of two samples look identical, however a careful look brings out some subtle differences which are important to characterize the magnetic ground state of these compositions. The magnetic contribution to the specific heat (C_{mag}) has been calculated by subtracting the lattice contribution (C_{latt}) from total heat capacity C . Here C_{latt} has been estimated from the heat capacity data of isostructural non-magnetic compound LiCoO_2 taken from reference³² followed by proper scaling as prescribed by Bouvier *et al*³³. The main panel of fig. 4(a)

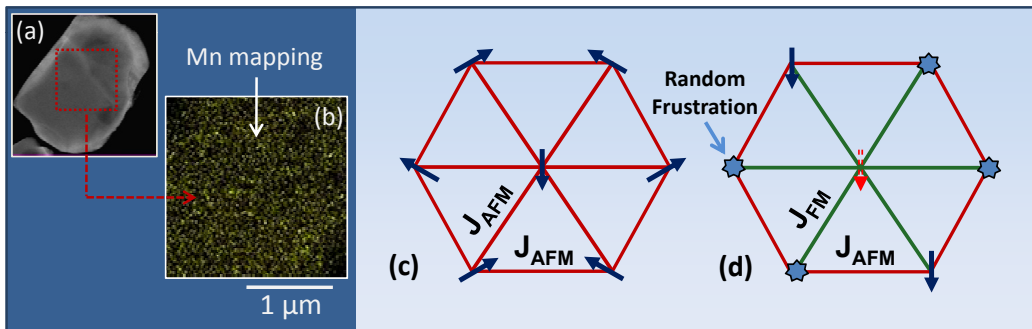


FIG. 5. (a) shows TEM image of an Mn10 crystallite. (b) illustrates element mapping on the selected region of the same particle using high resolution transmission electron microscope with bright spots denoting Mn. (c) represents cartoon of a frustrated triangular lattice with nearest neighbor AFM interaction and 120° noncollinear AFM order. (d) depicts how the generation of random FM bonds by means of doping (dashed spin) can destroy the ordering.

(left axis) shows the C_{mag}/T versus T plot. T_N in both the samples are seen as a broad peak around 45 K (this resembles well with the reported C_{mag}/T versus T data of pure LiCrO_2 ¹³). A marked difference is observed between C_{mag}/T data of Mn10 and Ga10 below T_N . For Ga10, C_{mag}/T smoothly decreases with decreasing T , whilst C_{mag}/T shows a shoulder like feature below about 14 K in Mn10. This feature matches well with the FC-ZFC bifurcation temperature T_{irr} in the $M(T)$ data of the same sample.

We have carefully examined the low temperature part of C_{mag} of both the samples as depicted in fig. 4(b). A higher value of C_{mag} is observed for the Mn10 sample. In Mn10, the larger value of the magnetic entropy (S_{mag}) calculated from C_{mag} (see inset of fig. 4(b)) is related to the excess magnetic disorder. For an AFM sample with linear $\omega - q$ dispersion relation of magnons, one expects C_{mag} to vary as T^3 at low- T . A predominant T^3 dependent C_{mag} is found for Ga10, which signifies an ordered AFM state. We have fitted the observed C_{mag} data of Mn10 and Ga10 samples using the relevant algebraic expressions and it brings out some novel information regarding their respective magnetic ground states. For Ga10, it is found that a simple T^3 is unable to provide a good fit to C_{mag} below 14 K. Rather an equation $C_{mag} = a_1 T + a_3 T^3$ provides the best fit to the data with $a_1 = 3.6 \text{ mJ}(\text{mol})^{-1}\text{K}^{-2}$ and $a_3 = 9.77 \times 10^{-2} \text{ mJ}(\text{mol})^{-1}\text{K}^{-4}$. Since these samples are highly insulating, an electronic origin of linear T term in C_{mag} can be ruled out. Such linear T term is likely to have magnetic origin and probably it denotes some disordered magnetic state.

Now turning to Mn10, C_{mag} shows a linear behavior below 14 K, which corresponds an SG state (since the sample is an insulator)³⁴. An upward curvature is observed below about 3 K in the $C_{mag}(T)$ data of Mn10. The linear part between 12 and 3 K, if extrapolated, hits the abscissa at a positive finite value of T . Such finite intercept and low- T curvature are previously observed in several canonical SGs^{21,34}. C_{mag} between 12 and 3 K was

fitted by an algebraic formula $C_{mag} = b_0 + b_1 T$ with $b_0 = -127.66 \text{ mJ}(\text{mol})^{-1}\text{K}^{-1}$ and $b_1 = 55.25 \text{ mJ}(\text{mol})^{-1}\text{K}^{-2}$.

The SG state in Mn10 sample is of reentrant type, which develops out of an AFM ordered state. Occurrence of reentrant spin glass (RSG) in AFM system, albeit fewer in number than its FM counterpart, are well documented in the literature³⁵⁻³⁸. It has been argued that $\text{Mn}^{3+}\text{-Cr}^{3+}$ interaction can be FM type particularly when the metal atoms are in octahedral oxygen environment³⁹⁻⁴³. Substitution of Mn at the Cr site can give rise to random FM bonds in the otherwise 120° non-co-linear AFM structure of LiCrO_2 (see fig. 5). In the random field model of RSG as proposed by Aeppli *et al.*,⁴⁴ presence of spatially uncorrelated conflicting magnetic bonds can destroy the long range FM ordering through the emergence of random microscopic field. The system then attains a frozen non-ergodic state similar to conventional spin glasses. An equivalent scenario can occur when an AFM ordering is destroyed resulting a reentrant glassy state, which would be appropriate for the present Mn-doped LiCrO_2 sample. Similar argument was actually provided in case of AFM spin glass observed in Cr doped manganites³⁵.

A cartoon of the 120° AFM spin arrangement on a 2D hexagonal lattice is depicted in fig. 5(c). Substitution of one magnetic impurity (dashed spin in fig. 5(d)) at the center of the hexagon with nearest neighbor FM interaction (similar to Cr-Mn FM bond in Mn doped LiCrO_2) can destroy the ordering arrangement through the development of conflicting sense of interactions. If such substitutions are spatially random, the system will never attain an order arrangements of spins (like the regular GF system without quenched disorder) and may lead to a glassy state.

It has long been argued whether the ground state of an RSG system is truly spin glass like or SG state coexists with the long range ordered state⁴⁵⁻⁴⁸. Unlike Ga10, we do not observe any T^3 term in the C_{mag} versus T (expected for an AFM state) plot below 14 K of Mn10. This indicates that the ground state of Mn10 is truly SG

type without any coexisting AFM component. Doping of magnetic atoms often results superparamagnetic like phase due to the clustering of dopant atoms (as in Cu-Mn or Au-Fe alloys²²). In that case one would expect a $T^{3/2}$ term in the C_{mag} versus T plot due to intra-cluster FM coupling.⁴⁹ A clear linear variation of C_{mag} in Mn10 ruled out the possibility of any superparamagnetic clustering effect. We physically examined the sample using high resolution transmission electron microscope for element mapping, where the spatial distribution of the elements present in the sample can be observed. Our data (see fig. 5) does not indicate any clustering of Mn atoms even down to the nanometer scale. It is generally believed that a true RSG state exists only in a magnetic system below three dimension⁴⁵ and thus Mn10 can be regarded as a novel example of such complete reentry for its layered quasi-2D structure.

IV. CONCLUSION

We would like to conclude by comparing our result with the recently published work on doped ZnCr_2O_4 , where a quasi-spin glass state is observed on small amount (1% to 5%) of Ga doping⁵⁰. The quasi spin glass state is characterized by thermomagnetic irreversibility and a linear term in the C versus T data. The authors argued that the substitution of Ga at the Cr site creates *quasi-spins* which give rise to some degree of non-ergodicity. For our case even 10% Ga doping does not give rise to a true spin glass state. However, it should be noted that a linear- T part is indeed present on top of the cubic part in C_{mag} of

Ga10. The coefficient of linear term is $3.6 \text{ mJ}(\text{mol})^{-1}\text{K}^{-2}$ which is substantially smaller than the linear term in Ga doped ZnCr_2O_4 (9.6 and $47.6 \text{ mJ}(\text{mol})^{-1}\text{K}^{-2}$ on 1% and 5% Ga doping respectively). Ga10 is certainly not a spin glass, but it resembles to some extent with the quasi spin glass state reported in doped ZnCr_2O_4 . Both LiCrO_2 and ZnCr_2O_4 are GF magnetic systems, although they are quite different as far as the crystal structure (layered and cubic spinel respectively) and dimension of magnetic interaction (quasi-2D and 3D respectively) are concerned. ZnCr_2O_4 undergoes first order phase transition paving the path for disorder through strain field distribution^{51,52}. These factor may enhances the chances of added metastability in case of Ga doped ZnCr_2O_4 .

Summarizing, a true SG state is only observed in LiCrO_2 on Mn doping at Cr site, whilst similar Ga doping does not lead to an SG state. The 10% Mn-doped sample shows a true reentrance of SG phase in an otherwise AFM state. It appears that random magnetic impurities are essential for the development of an glassy magnetic state in this GF compound. This is quite different from the case of other GF systems where very small non-magnetic impurity can turn the system to a glassy phase. Therefore, it seems that there is no generalized rule for the development of glassy state in a GF system.

SC wishes to thank CSIR (India) for his research studentship. The funding from CSIR (grant number: 03(1209)/12/EMR-II) for the present work is thankfully acknowledged. The authors also like to thank the Low Temperature & High Magnetic Field (LTHM) facilities at UGC-DAE CSR, Indore (sponsored by DST) for heat capacity measurements.

* sspsm2@iacs.res.in

¹ J. E. Greedan, J. Mater. Chem. **11**, 37 (2001).

² A. P. Ramirez, Czech. J. Phys. **46**, 3247 (1996).

³ A. Harrison, J. Phys.: Condens. Matter **16**, S553 (2004).

⁴ A. P. Ramirez, Annu. Rev. Mater. Sci. **24**,453 (1994).

⁵ A. P. Ramirez, G. P. Espinosa, and A. S. Cooper, Phys. Rev. Lett. **64**, 2070 (1990).

⁶ P. Schiffer, A. P. Ramirez, D. A. Huse, P. L. Gammel, U. Yaron, D. J. Bishop, and A. J. Valentino, Phys. Rev. Lett. **74**, 2379 (1995).

⁷ M. J. P. Gingras, C. V. Stager, N. P. Raju, B. D. Gaulin, and J. E. Greedan, Phys. Rev. Lett. **78**, 947 (1997).

⁸ D. Fiorani, S. Viticoli, J. L. Dormann, J. L. Tholence, and A. P. Murani, Phys. Rev. B **30**, 2776 (1984).

⁹ W. Ratcliff II, S. -H. Lee, C. Broholm, S. -W. Cheong, and Q. Huang, Phys. Rev. B **65**, 220406 (2002).

¹⁰ A. Andreanov, J. T. Chalker, T. E. Saunders, and D. Sherrington, Phys. Rev. B **81**, 014406 (2010).

¹¹ D. K. Singh and Y. S. Lee, Phys. Rev. Lett. **109**, 247201 (2012).

¹² S.-H. Lee, C. Broholm, G. Aeppli, A. P. Ramirez, T. G. Perring, C. J. Carlile, M. Adams, T. J. L. Jones and B. Hessen, Europhys. Lett. **35**, 127 (1996).

¹³ L. K. Alexander, N. Büttgen, R. Nath, A. V. Mahajan,

and A. Loidl, Phys. Rev. B **76**, 064429 (2007).

¹⁴ J. Sugiyama, M. Månsson, Y. Ikeda, T. Goko, K. Mukai, D. Andreica, A. Amato, K. Ariyoshi, and T. Ohzuku, Phys. Rev. B **79**, 184411 (2009).

¹⁵ S. Seki, Y. Onose, and Y. Tokura, Phys. Rev. Lett. **101**, 067204 (2008).

¹⁶ A. Olariu, P. Mendels, F. Bert, L. K. Alexander, A. V. Mahajan, A. D. Hillier, and A. Amato, Phys. Rev. B **79**, 224401 (2009).

¹⁷ K. Dey, S. Majumdar and S. Giri, Phys. Rev. B **87**, 094403 (2013).

¹⁸ H. Kadowaki, H. Takei, and K. Motoya, J. Phys.: Condens. Matter **7**, 6869 (1995).

¹⁹ Y. Motoyama, H. Eisaki, and S. Uchida, Phys. Rev. Lett. **76**, 3212 (1996).

²⁰ S. Chattopadhyay, S. Giri, and S. Majumdar, J. Phys.: Condens. Matter **23**, 216006 (2011).

²¹ K. Binder and A. P. Young, Rev. Mod. Phys. **58**, 801 (1986).

²² J. A. Mydosh, *Spin Glasses: An Experimental Introduction* (Taylor & Francis, 1993).

²³ J. C. Phillips, Rep. Prog. Phys. **59**, 1133 (1996).

²⁴ R. V. Chamberlin, G. Mozurkewich, and R. Orbach, Phys. Rev. Lett. **52**, 867 (1984).

- ²⁵ R. S. Freitas, L. Ghivelder, F. Damay, F. Dias, and L. F. Cohen, *Phys. Rev. B* **64**, 144404 (2001).
- ²⁶ F. Wang, J. Zhang, Y. -f. Chen, G. -j. Wang, J. -r. Sun, S. -y. Zhang, and B. -g. Shen, *Phys. Rev. B* **69**, 094424 (2004).
- ²⁷ D. Chu, G. G. Kenning, and R. Orbach, *Phys. Rev. Lett.* **72**, 3270 (1994).
- ²⁸ A. Bhattacharyya, S. Giri, and S. Majumdar, *Phys. Rev. B* **83**, 134427 (2011).
- ²⁹ S. Chattopadhyay, S. Jana, S. Giri, and S. Majumdar, *J. Phys.: Condens. Matter* **24**, 436005 (2012).
- ³⁰ M. Sasaki, P. E. Jonsson, H. Takayama, and H. Mamiya, *Phys. Rev. B* **71**, 104405 (2005).
- ³¹ Y. Sun, M. B. Salamon, K. Garnier, and R. S. Averback, *Phys. Rev. Lett.* **91**, 167206 (2003).
- ³² H. Kawaji, M. Takematsu, T. Tojo, T. Atake, A. Hirano and R. Kanno, *J. Thermal analysis and calorimetry* **68**, 833 (2002).
- ³³ M. Bouvier, P. Lethuillier, and D. Schmitt, *Phys. Rev. B* **43**, 13137 (1991).
- ³⁴ D. L. Martin, *Phys. Rev. B* **20**, 368 (1979).
- ³⁵ J. Dho, W. S. Kim, and N. H. Hur, *Phys. Rev. Lett.* **89**, 027202 (2002).
- ³⁶ W. R. Chen, F. C. Zhang, J. Miao, B. Xu, X. L. Dong, L. X. Cao, X. G. Qiu, B. R. Zhao, and P. Dai, *Appl. Phys. Lett.* **87**, 042508 (2005).
- ³⁷ X. Zhang, S. Tang, Y. Li, and Y. Du, *Phys. Lett. A* **374**, 2175 (2010).
- ³⁸ S. Nimori and D. Li, *J. Phys. Soc. Jpn.* **75**, 195 (2006).
- ³⁹ G. H. Jonker, *Physica* **22**, 707 (1956).
- ⁴⁰ Y. Sun, W. Tong, X. Xu, and Y. Zhang, *Phys. Rev. B* **63**, 174438 (2001).
- ⁴¹ X. Xiao, S. L. Yuan, Y. Q. Wang, G. M. Ren, J. H. Miao, G. Q. Yu, Z. M. Tian, L. Liu, L. Chen, and S. Y. Yin, *Solid State Commun.* **141**, 348 (2007).
- ⁴² J. Deisenhofer, M. Paraskevopoulos, H. -A. K. von Nidda, and A. Loidl, *Phys. Rev. B* **66**, 054414 (2002).
- ⁴³ R. Ganguly, I. K. Gopalakrishnan, and J. V. Yakhmi, *Physica B* **275**, 308 (2000).
- ⁴⁴ G. Aeppli, S. M. Shapiro, R. J. Birgeneau, and H. S. Chen, *Phys. Rev. B* **28**, 5160 (1983).
- ⁴⁵ K. Jonason, J. Mattson and P. Nordblad, *Phys. Rev. B* **53**, 6507 (1996).
- ⁴⁶ I. Mirebeau, S. Itoh, S. Mitsuda, T. Watanabe, Y. Endoh, M. Hennion, and R. Papoular, *Phys. Rev. B* **41**, 11405 (1990).
- ⁴⁷ T. H. Kim, M. C. Cadeville, A. Dinia, and H. Rakoto, *Phys. Rev. B* **53**, 221 (1996).
- ⁴⁸ S. Niidera and F. Matsubara, *Phys. Rev. B* **75**, 144413 (2007).
- ⁴⁹ J. O. Thomson, and J. R. Thompson, *J. Phys. F: Metal Phys.* **11**, 247 (1981).
- ⁵⁰ A. D. LaForge, S. H. Pulido, R. J. Cava, B. C. Chan, and A. P. Ramirez, *Phys. Rev. Lett.* **110**, 017203 (2013).
- ⁵¹ I. Kagomiya, H. Sawa, K. Siratori, K. Kohn, M. Toki, Y. Hata, and E. Kita, *Ferroelectrics* **268**, 327 (2002).
- ⁵² S. -H. Lee, C. Broholm, T. H. Kim, W. Ratchiff II, and S. -W. Cheong, *Phys. Rev. Lett.* **84**, 3718 (2000).